Contacting individual Fe(110) dots in a single electron-beam lithography step

Fabien Cheynis, Helge Haas, Thierry Fournier, Laurent Ranno, Wolfgang Wernsdorfer, Olivier Fruchart, Jean-Christophe Toussaint

▶ **To cite this version:**

Fabien Cheynis, Helge Haas, Thierry Fournier, Laurent Ranno, Wolfgang Wernsdorfer, et al.. Contacting individual Fe(110) dots in a single electron-beam lithography step. 2008. hal-00276721v1

HAL Id: hal-00276721

https://hal.science/hal-00276721v1

Preprint submitted on 30 Apr 2008 (v1), last revised 23 Feb 2009 (v2)

HAL is a multi-disciplinary open access archive for the deposit and dissemination of scientific research documents, whether they are published or not. The documents may come from teaching and research institutions in France or abroad, or from public or private research centers.

L'archive ouverte pluridisciplinaire **HAL**, est destinée au dépôt et à la diffusion de documents scientifiques de niveau recherche, publiés ou non, émanant des établissements d'enseignement et de recherche français ou étrangers, des laboratoires publics ou privés.

Contacting individual Fe(110) dots in a single electron-beam lithography step

F. Cheynis,[1,2,*] H. Haas,[1] T. Fournier,[1] L. Ranno,[1] W. Wernsdorfer,[1] O. Fruchart,[1,†] and J.-C. Toussaint[1,2]

[1] *Institut NÉEL, CNRS-UJF, BP 166, F-38042 Grenoble Cedex 9, France*
[2] *INPG, 46 avenue Félix Viallet, F-38031 Grenoble Cedex 1, France*

(Dated: April 30, 2008)

We report on a new approach, entirely based on electron-beam lithography technique, to contact electrically, in a four-probe scheme, single nanostructures obtained by self-assembly. This technique has been developed to study the field-induced reversal of an internal component of an *asymmetric Bloch* domain wall observed in elongated structures such as Fe(110) dots. We have focused on the control, using an external magnetic field, of the magnetisation orientation within *Néel caps* that terminate the domain wall at bot interfaces. Preliminary magneto-transport measurements are discussed demonstrating clearly that a single Fe(110) dot has been contacted.

PACS numbers: 73.63.Rt,81.16.Dn,75.60.Ch, 75.60.Jk, 75.30.Gw

Micromagnetic configuration control in nanostructures has generated numerous studies over the last few years as data storage applications using more than one bit per memory element seem now reachable. So far, most of the published works have focused on the vortex configuration observed for instance in circular dots[1]. The control of the magnetisation vortex core orientation using a magnetic field either out-of-plane[2, 3] or in-plane[4, 5] or using an AC current[6] has been widely studied. Recently we have demonstrated that an *asymmetric Bloch wall* that can be considered has a sheared vortex and observed in elongated structures (in our case self-assembled Fe(110) dots) exhibited a supplementary degree of freedom that can be controlled using a magnetic field[7, 8]. The magnetisation orientation within the two Néel caps that terminate the asymmetric Bloch wall at both interfaces in elongated structures defines this additional degree of freedom. To observe in real-time the Néel cap reversal and demonstrate experimentally its associated hysteresis, we opted for an approach based on magneto-transport on individual structures. We have thus designed a four-probe measurement pattern to study individual metallic structures of low impedance. This pattern consists of two bottom electrodes and two top electrodes electrically isolated by a dielectric layer. This layer has to be etched precisely on top of a selected Fe(110) dot per pattern. The signal used to probe the Néel cap reversal is the *Anisotropic Magneto-Resistance* (AMR) which yields to different resistance states for a transverse (*i.e.* along the width of the Fe(110) dots) current component.

In this letter, we report on a new technique, entirely based on electron-beam (e-beam) lithography, to carry out four-probe measurements of self-assembled Fe(110) dots. We opted for a simple approach that can be applied as a general procedure to contact other self-assembled nanostructures randomly distributed over sample surface. More particularly, our innovative approach made it possible to circumvent the technical difficulties which consist in localising precisely self-assembled structures and in contacting selected dots. In our method, we addressed these two crucial issues in a single e-beam lithography step. Preliminary magneto-resistance (MR) measurements of individual Fe(110) dots will be then discussed as a proof of the reliability of our approach.

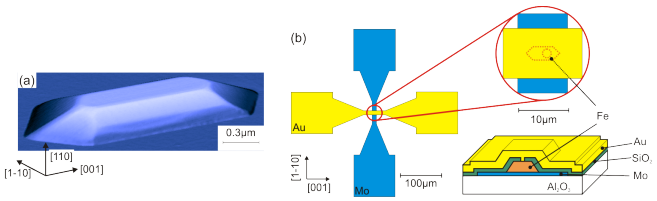

FIG. 1: (a) AFM image of a typical Fe(110) dot obtained by PLD (Ref. [7]). (b) Schematic illustration of the four-probe design with the bottom (Mo) and top (Au) electrodes. These electrodes are electrically isolated by a SiO_2 layer deposited on the Au coverage layer. The dielectric layer has to be etched on top of an individual selected Fe(110) dot in the central area of the pattern.

Fe(110) dots are obtained by Pulsed-Laser Deposition (PLD) under Ultra-High Vacuum conditions[9]. These structures are deposited on an epitaxial Mo(110) or W(110) buffer layer which has been previously deposited on a sapphire $(11\bar{2}0)$ substrate. The Stranski-Krastanov growth of the Fe dots is obtained for a deposition temperature in the range ∼600-850 K [Fig. 1(a)]. For our study, the Fe dots have been deposited at ∼800 K on a 50 nm Mo(110) buffer layer and covered by a ∼0.7 nm Mo layer and a 5 nm Au layer to prevent from oxydation.

The sample has been processed using a SEM-FEG *LEO 1530* remote-controlled by the *Elphy plus* system (*Raith GmbH*) for e-beam lithography. A schematic view of our pattern is presented in Fig. 1(b). The first step of our process is based on a routine procedure using *Shipley UVN2®* chemically amplified negative resist for the fabrication of the bottom electrodes

*Present adress : Laboratoire de Photonique et de Nanostructures - CNRS, Route de Nozay, 91460 Marcoussis, France
†olivier.fruchart@grenoble.cnrs.fr

in the Mo(110) buffer layer by Ar Ion Beam Etching (ϕ_{Ar} = 3.3 cm^3/min). The 230 nm resist mask is thick enough to protect ∼140 nm Fe(110) dots upon etching process of the 50 nm Mo(110) buffer layer. Once the UVN2 layer removed using *EKC*® *LE*® solution, a 55 nm SiO_2 layer has been deposited on the sample surface using RF Magnetron sputtering technique.

The next step of our process consists in patterning the SiO_2 layer on top of selected Fe(110) dots (ϕ = 100 nm and ϕ = 200 nm holes) and on top of the bottom contact pads using a *Microchem PMMA* positive resist layer as a mask. Our most significant breakthrough has been to develop an exposure procedure to localise and contact individual Fe(110) dots in a single e-beam step. Our approach is based on the imaging of the central area of the pattern covered with a PMMA resist layer and a 10 nm Al layer. A single Fe(110) dot per pattern is then selected and exposed in the very same process step. Note that the Al layer makes it possible to image the surface of the sample covered with an insolating PMMA layer. The technical difficulty of this step has been to optimise the quality of the image used to determine the structure to be connected without exposing the electron sensitive PMMA resist in a too significant manner. In our process, two images are required to shift e-beam writefields with a sufficient accuracy (¡150 nm) on top of the selected structure. We have used a standard 180 nm PMMA 3 % layer spin-coated on a so-called *test* sample exhibiting ∼120 nm Fe(110) dots to optimise imaging conditions [Fig. 2]. The key parameters are the size (in μm) and the resolution (in px) of each image. These parameters define, knowing the beam current and the dwell-time per pixel, an equivalent exposure dose (EED). The SEM imaging of Fe(110) dots is possible because the PMMA\Al surface is not perfectly flat on top of Fe(110) dots. Typically, 30-40 nm-high prominences have been observed using AFM in contact mode. The thickness of the PMMA layer on top of Fe(110) dots is thus ∼80 nm.

After imaging, selection, exposure and development steps, contact AFM images of the PMMA layer have been recorded to quantify the effect of SEM image acquisition on the resist thickness and to check the accuracy of the e-beam writefields' shifts [Fig. 2(b-c)]. It turns out that the first 15 μm×15 μm SEM picture (256 px×256 px), labeled **1** in Fig. 2(b), consumes only 3 nm of the resist layer while in the overlapping area with the second SEM image, labeled **2** in Fig. 2(b), ∼30 nm of PMMA have been removed. The remaining thickness of the PMMA layer on top of each exposed Fe(110) dot is thus 50 nm, which turned out to be sufficient to protect the rest of the exposed Fe(110) dots as explained below. The EED of both images is ∼27 μC/cm^2, that is a total EED of ∼54 μC/cm^2, which is significantly below typical exposure dose values of 450-600 μC/cm^2 used for PMMA resist layers. Fig. 2(c) highlights the fact that exposure position accuracy better than 150 nm are obtained. From this image, the thickness of the exposed area on top of a Fe(110) dot can be estimated at ∼70 nm. This thickness

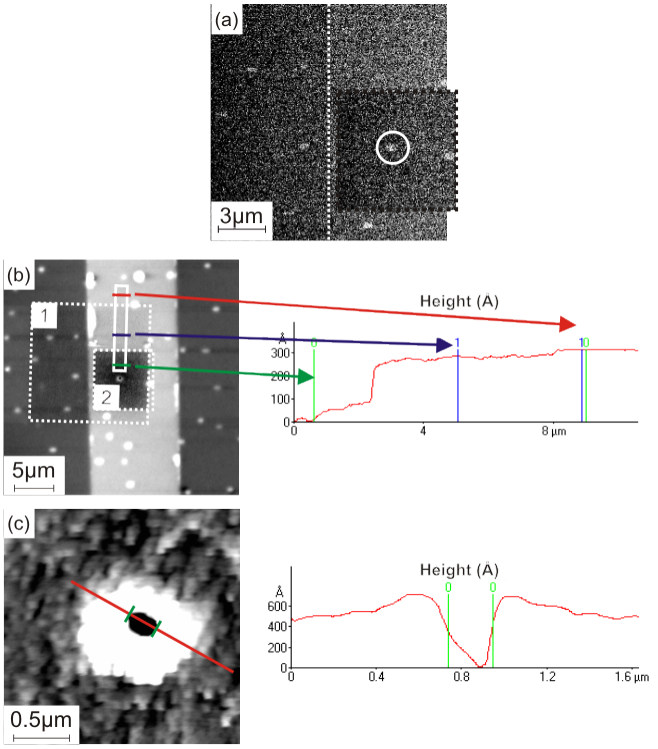

FIG. 2: Optimised imaging conditions of the central area of our pattern. (a) SEM images of the sample surface covered by a PMMA resist layer and a 10 nm Al layer. These images have been used to shift the e-beam writefields on top of a selected Fe(110) dot (white circle). The dashed white line is a guide-to-the-eye for the limit of the bottom contacts. (b-c) Contact AFM images of the central area of the *test* sample obtained after imaging, selection, exposure and development steps. Image (b) makes it possible to quantify the effect of imaging the PMMA\Al surface on the resist thickness. Image (c) highlights the position accuracy of the exposure step and the dimensions of the exposed area.

is however underestimated owing to the finite tip radius (typically 10 nm) and the full tip cone angle (typically 40 ®). This means that it can be concluded from this measurement that the resist layer has been completely exposed on top of the selected Fe(110) dots. It also turns out that the FWHM of the exposed circle is of the order of 205 nm which is good agreement with a diameter setpoint of 200 nm. Finite size tip effects are also expected to underestimate this value.

For the sample exhibiting ∼140nm nm Fe(110) dots, we have used a thicker resist layer (PMMA 4 %, 240 nm). Although the PMMA 4 % layer has been observed to be more sensitive to e-beam exposure, similar protection conditions of the ∼140nm nm Fe(110) dots have been obtained.

Once developed, the PMMA resist layer serves as a mask for a Reactive Ion Etching of the SiO_2 layer using a CHF_3 RF plasma ($P_{CHF_3} = 2.10^{-2}$ Torr, P_{RF} = 50 W). The etching has been monitored using a laser reflectometry setup on a Si\SiO_2 layer deposited at the same

time to that covering Fe(110) dots. For the test sample exhibiting ∼120 nm Fe(110) dots, the etching process has been intentionally prolongated. Fig. 3(a) shows the effects of this extended etching step on the Fe(110) dot surface. More particularly, it clearly demonstrates that only the exposed area is affected by the etching process, leaving the rest of the top Fe(110) dot surface unaffected. The last step of our process is a standard lift-off technique of a Ti\Au (10 nm\100 nm) layer using automatic realignment procedure and a PMMA positive resist [3(b)]. The structured Ti\Au layer defines the top electrodes and connects a single Fe(110) dot per pattern and the bottom electrodes.

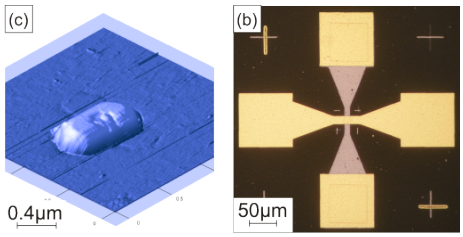

FIG. 3: (a) Contact mode AFM image of a Fe(110) dot after an extended etching process. (b) Optical image of the final pattern highlighting bottom (grey) and top (yellow) contacts.

Magneto-transport measurements have been carried out in a temperature variable (2.2 K-300 K) pumped He cryostat. In-plane magnetic field up to 7 T is provided by a superconducting magnet. Sample holder can be rotated continuously in-the-plane of the sample. In our measurements, we have used two applied field configurations with respect to Fe(110) dots' orientation : along the [001] (*longitudinal*) direction and along the [1$\bar{1}$0] (*transverse*) direction. Low-noise/low-impedance (∼1 Ω) setup has been developed using a *Stanford Research Systems SR830* lock-in device and a high-impedance polarisation charge (1 kΩ) as a current source [Fig. 4(a)]. Four-probe sample voltage is then detected at the lock-in frequency [Fig. 4(b)].

Zero-field resistance of a pattern is plotted in Fig. 5 as a function of sample temperature. It clearly exhibits a behaviour proportional to $\sim 1/T$ from ∼1.6 Ω at room temperature (RT) down to ∼1.1 Ω at 50-70 K where it reaches a residual value. This demonstrates that a metallic contact has been established between the top and bottom electrodes. This metallic contact cannot be attributed to a leakage through the dielectric layer which has been observed to yield to higher contact resistances (∼50 Ω) for samples used to develop our process. Electrocinetic simulations carried out using *COMSOL Multiphysics* software made it possible to determine characteristic resistances using RT bulk resistivities of the different materials. It turns out that resistances of 0.3 Ω and 0.2 Ω are expected from the Au contact cylinder on top of the connected Fe(110) dot and from this very same Fe(110) dot, respectively. Despite working in a four-probe configuration, a resistance of 0.5 Ω in the Mo layer is predicted by electrocinetic simulations. Lead resistance of the same order of magnitude is expected in the Au layer yielding to a total extra resistance of ∼1.3 Ω. Lead resistance in low-impedance structures is known as *current-crowding*[10]. Using Eq. (7) in Ref. [10], we find an additional lead resistance of ∼1.4 Ω. In both cases, the predicted four-probe resistance is in quantitative agreement with experimental value. This validates that a single Fe(110) dot has been connected. The small decrease of the device resistance between room temperature and 2.2 K (∼30 %) also confirms that a significant contribution to our signal can be attributed to the Au layer defining top electrodes. Single crystalline Mo(110) resistance has been indeed observed to decrease by a factor 25 between RT and the low-temperature regime.

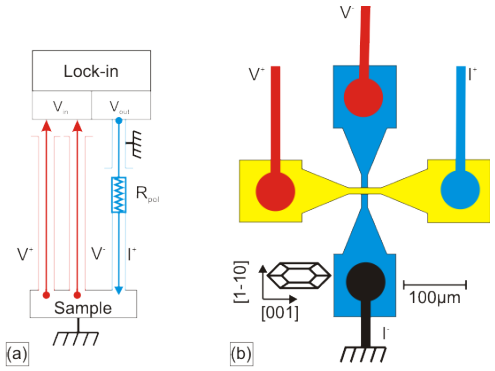

FIG. 4: Schematic illustrations of our magneto-transport setup. (a) A *Stanford Research Systems SR830* lock-in device and a high-impedance polarisation charge (1 kΩ) are used to inject an AC current of constant amplitude into a single Fe(110) dot. Four-probe sample voltage is measured at the lock-in frequency. (b) Four-probe contacts of a pattern.

Typical low-temperature MR measurements obtained for longitudinal and transverse fields are shown in Fig. 5(b-c). Fig. 5(b) clearly exhibits a Lorentz-like MR (*i.e.* $\sim B^2_{\text{app}}$) despite a counter-intuitive negative component. The origin of this negative MR remains an open question. We have also observed peaks in the MR response only for transverse applied fields [Fig. 5(c)]. More particularly, the minima measured at $\sim \pm 0.4$ T may be attributed to the transverse saturation of the Fe(110) dots in a quantitative agreement with previous data obtained using Vibrating Sample Magnetometry for an assembly of Fe(110) dots[11]. The two maxima observed at $\sim \pm 0.2$ T . The origin of the high-field MR differences observed in Fig. 5(d) and Fig. 5(e) which have been obtained under identical conditions . From Fig. 5(d-e), no clear evidence of the existence of an hysteresis associated with Néel cap reversal can be drawn. However, time-averaged measurements may help to observe this hysteresis by improving our signal-to-noise ratio.

In conclusion, we have developed a new approach

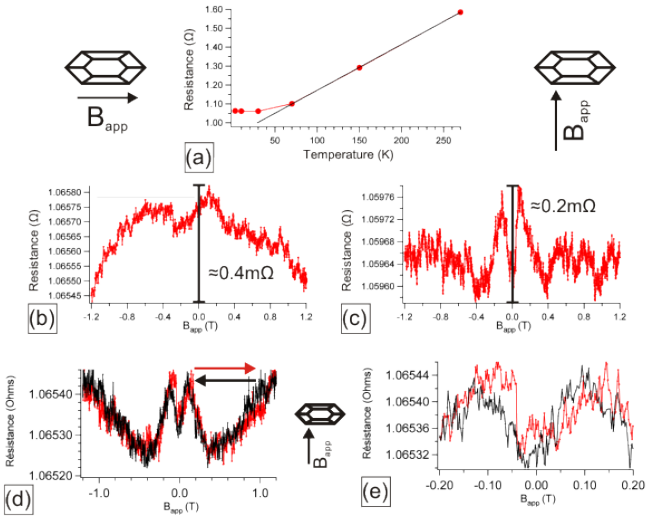

FIG. 5: (a) Zero-field resistance of a single Fe(110) dot as a function of sample temperature. (b-d) Magneto-resistance of a single Fe(110) dot for (b) longitudinal and (c) transverse applied field directions. (d) Complete field-scan (back and forth between -1.2 T and +1.2 T) magneto-resistance of a single Fe(110) dot under a transverse magnetic field. (e) Zoom-in of (d) in the [-0.2 T; +0.2 T] range. For all measurements, typical injection current is ~ 1 mA.

to contact, in a single e-beam lithography step, self-assembled nanostructures. This technique has been developed to study the field-induced reversal of an internal degree of freedom of an asymmetric Bloch wall (*i.e.* the orientation of Néel caps) in individual Fe(110) dots. Preliminary MR results obtained confirm that individual Fe(110) dots have been connected. Despite remaining open questions, we have observed peaks in the MR response only for transverse applied fields. The mimina can be attributed to the transverse saturation of the Fe(110) dots and the maxima are likely to be the signature of the Néel cap reversal.

Acknowledgments

We are grateful to P. David and V. Santonacci (sample elaboration), T. Crozes (nanofabrication), D. Dufeu and D. Maillard (magneto-transport) for technical support and fruitful discussions.

[1] T. Shinjo, T. Okuno, R. Hassdorf, K. Shigeto, and T. Ono, Science **289**, 930 (2000).
[2] T. Okuno, K. Shigeto, T. Ono, K. Mibu, and T. Shinjo, J. Magn. Magn. Mater. **240**, 1 (2002).
[3] A. Thiaville, J. M. García, R. Dittrich, J. Miltat, and T. Schrefl, Phys. Rev. B **67**, 094410 (2003).
[4] B. Van Waeyenberge, A. Puzic, H. Stoll, K. W. Chou, T. Tyliszczak, R. Hertel, M. Fähnle, H. Brückl, K. Rott, G. Reiss, et al., Nature **444**, 461 (2006).
[5] R. Hertel, S. Gliga, C. Schneider, and M. Fähnle, Phys. Rev. Lett. **98**, 117201 (2007).
[6] K. Yamada, S. Kasai, Y. Nakatani, K. Kobayashi, H. Kohno, A. Thiaville, and T. Ono, Nat. Mater. **6**, 270 (2007).
[7] F. Cheynis, N. Rougemaille, R. Belkhou, J.-C. Toussaint, and O. Fruchart, J. Appl. Phys. **103**, 07D915 (2008).
[8] F. Cheynis, O. Fruchart, J.-C. Toussaint, N. Rougemaille, and R. Belkhou, Science (2008), submitted.
[9] O. Fruchart, P.-O. Jubert, M. Eleoui, F. Cheynis, B. Borca, P. David, V. Santonacci, A. Liénard, M. Hasegawa, and C. Meyer, J. Phys.: Condens. Matter **19**, 053001 (2007).
[10] J. Chen, Y. Li, J. Nowak, and J. F. de Castro, J. Appl. Phys. **91**, 8783 (2002).
[11] P.-O. Jubert, Ph.D. thesis, Université Joseph Fourier - Grenoble I (2001), URL http://tel.archives-ouvertes.fr/docs/00/04/58/68/PDF/tel-00004054.pdf.